Middle-East Journal of Scientific Research 24 (12): 3838-3857, 2016
ISSN 1990-9233

DOI: 10.5829/idosi.mejsr.2016.3838.3857

Ancillary Service Requirement Assessment Indices Evaluation with Proportional and Integral plus Controller in a Restructured Power System with Hydrogen Energy Storage Unit

K. Chandrasekar, B. Paramasivam and I.A. Chidambaram

Department of Electrical Engineering, Annamalai University, Annamalainagar, Tamilnadu, India

Abstract: This paper proposes the computation procedure for obtaining Power System Ancillary Service Requirement Assessment Indices (PSASRAI) for a Two-Area Thermal Reheat Interconnected Power System (TATRIPS) in a restructured environment. These indices indicate the Ancillary Service Requirement to improve the efficiency of the physical operation of the power system. Even though Proportional and Integral (PI) type controllers have wide usages in controlling the Load-Frequency Control (LFC) problems the Integral gain in the PI controller is limited relatively to small values because of its high the overshoot in the transient's response. So the Proportional and Integral plus (PI^+) controller was proposed and adopted in this paper. The PI^+ controller gains values for the restructured power system are obtained using Bacterial Foraging Optimization (BFO) algorithm. The PSASRAI are computed based on the settling time and peak over shoot of the control input deviations of each area. To ensure a faster settling time and reduced peak over shoot of the control input requirements, energy storage is an attractive option to adopt for the demand side management implementation. Hence Hydrogen Energy Storage (HES) unit was adopted effectively to TATRIPS to meet the peak demand. In this paper the PSASRAI are calculated for different types of transactions and the necessary remedial measures to be adopted are also suggested.

Key words: Ancillary Service · Hydrogen Energy Storage · Proportional and Integral plus Controller · Bacterial Foraging Optimization · Power System Ancillary Service Requirement Assessment Indices

INTRODUCTION

The successful operation of an interconnected power system requires not only in matching the total generation with total load demand but also to reduce the associated system losses. A small load fluctuation in any area causes the frequency deviation in all the areas and also of the tie-line power flow. These deviations have to be corrected through supplementary control which is referred as load-frequency Control (LFC) and the main objective of the LFC is to maintain the frequency and power interchanges within the interconnected control areas at the scheduled values [1, 2]. The restructuring and deregulation of power sector is to create a competitive environment where generation and transmission services are bought and sold under demand and supply market conditions [3]. In the deregulated power system, the power generating units are separated from transmission and distribution entities and all the power generating stations are recognized as Independent Power Producers (IPPs) or GENCOs [4] which will have a free market to compete each other to sell the electrical power. The retail consumers are supposed to buy the electrical power from the distribution companies which are referred as DISCOs. There are also third players between the GENCOs and DISCOs for wheeling the between them and are designated as TRANSCOs. So in the restructured environment the power system instead of having single vertical entity it will have three players viz GENCOs, DISCOs and TRANSCOs which can operate separately with their own set of functionalities. To supply the regulation between Disco and Genco, a contract will be established between these entities i.e. a distribution company has the freedom to have a contract with any

Corresponding Author: K. Chandrasekar, Department of Electrical Engineering, Annamalai University, Annamalainagar, Tamilnadu, India.

generation companies for purpose of transaction of power. The different companies may have the bilateral transactions and these will have to be monitored through an independent system operator which will control the number of ancillary services. The main task of the LFC is to maintain the reliability of the system at the desired frequency even for the varying load demand. The generation companies in restructured environment may or may not participate in the LFC task [5, 6]. As far as the optimal LFC schemes for interconnected power systems operating in deregulated environment are concerned, a considerable work has been reported in literature [2-9].

Ancillary services can be defined as a set of activities undertaken by generators, consumers and network service providers and coordinated by the system operator that have to maintain the availability and quality of supply. In a competitive power market, various service markets are adopted for ensuring the ancillary services such for voltage support, regulation, etc [10, 11]. The real power generating capacity related ancillary services, including Regulation Down Reserve (RDR), Regulation Up Reserve (RUR) in which regulation is the load following capability under Load Frequency Control (LFC). Spinning Reserve (SR) is a type of operating reserve, which is a resource capacity synchronized to the system that is unloaded, is able to respond immediately to serve load and is fully available within ten minutes. But Non Spinning Reserve (NSR) are the one in which NSR is not synchronized to the system and Replacement Reserve (RR) is a resource capacity non-synchronized to the system, which is able to serve load normally within thirty or sixty minutes. Reserves can be provided by generating units or interruptible load in some cases [11].

In this paper various procedures are adopted in computing Power System Ancillary Service Requirement Assessment Indices (PSASRAI) for a Two-Area Thermal Reheat Interconnected Power System (TATRIPS) in a restructured environment. The PSASRAI can be broadly classified as Feasible Assessment Indices (FAI) or Feasible Service Requirement Assessment Indices (FASRAI) and Comprehensive Assessment Indices (CAI) or Comprehensive Service Requirement Assessment Indices (CASRAI). From these indices the remedial measures to be taken can be adjudged like integration of additional spinning reserve, incorporation of effective intelligent controllers, load shedding etc.

In the early stages of power system restoration, the black start units are of great interest as they produce power for the auxiliaries of the thermal units without black start capabilities. Under this situation a conventional frequency control i.e., a governor may no longer be able to compensate for sudden the load changes due to its slow response. Therefore, in an inter area mode, damping out the critical electromechanical oscillations have to be damped out effectively by adopting efficient control methodologies in the restructured power system. Moreover, the system's control input requirement when monitored effectively and remedial actions to overcome the control input deviation excursions will protect the system before it enters an emergency mode of operation. Special attention is therefore given to the behavior of network parameters, control equipments as they affect the voltage and frequency regulation during the restoration process which in turn reflects in PSASRAI.

Most options proposed so far for LFC have not been implemented due to system operational constraints associated with thermal power plants. The main reason is the non-availability of required power other than the stored energy in the generator rotors, which can improve the performance of the system, in the wake of sudden increased load demands. In order to compensate the sudden load changes Hydrogen Energy Storage (HES) unit can be incorporated as it has a characteristic of ensuring an active power source with fast response in the power quality maintenance for decentralized power supplies. The HES systems have effective short-time overload output and have efficient response characteristics in the particular [12-14]. Now-a-days the complexities in the power system are being solved with the use of Evolutionary Computation (EC) such as Bacterial Foraging Optimization [BFO] which mimics how bacteria forage over a landscape of nutrients to perform parallel non-gradient optimization. The BFO algorithm is a computational intelligence based technique that is not affected larger by the size and nonlinearity of the problem and can be convergence to the optimal solution in many problems where most analytical methods fail to converge. This more recent and powerful evolutionary computational technique BFO [15-17] is found to be user friendly and is adopted for simultaneous optimization of several parameters for both primary and secondary control loops of the governor. In this study, BFO algorithm is used to optimize the Proportional and Integral plus (PI+) controller [18] gains for the load-frequency control of a Two-Area Thermal Reheat Interconnected Power System (TATRIPS) in a restructured environment with and without HES unit. Various case studies are analyzed to develop Power System Ancillary Service Requirement Assessment Indices (PSASRAI) namely, Feasible Assessment Index (FAI) and Comprehensive

Assessment Index (CAI) which are able to predict the modes of power system i.e., normal operating mode, emergency mode and restorative modes.

Modeling of a Two-Area Thermal Reheat Interconnected Power System (TATRIPS) in Restructured Scenario: With the emergence of the distinct identities of GENCOs, TRANSCOs, DISCOs and the ISO, many of the ancillary services of a Vertical Integrated Utility (VIU) will have a different role to play and hence have to be modeled differently. Among various ancillary service controls one of the most important services to be enhanced is the Load-Frequency Control (LFC). The LFC in a deregulated electricity market should be designed to consider different types of possible transactions, such as poolco-based transactions, bilateral transactions and a combination of these two [19]. In the new scenario, a DISCO can contract individually with a GENCO for acquiring the power and these transactions will be made under the supervision of ISO. To make the visualization of contracts easier, the concept of "DISCO Participation Matrix" (DPM) is used which essentially provides the information about the participation of a DISCO in contract with a GENCO. In DPM, the number of rows will be equal to the number of GENCOs and the number of columns will be equal to the number of DISCOs in the system. Any entry of this matrix is a fraction of total load power contracted by a DISCO toward a GENCO. As a results total of entries of column belong to DISCOi of DPM is $\Sigma_i cpf_{ij} = 1$. In this study two-area interconnected power system in which each area has two GENCOs and two DISCOs. Let $GENCO_1$, $GENCO_2$, $DISCO_1$, $DISCO_2$ be in area 1 and $GENCO_3$, $GENCO_4$, $DISCO_3$, $DISCO_4$ be in area 2 as shown in Fig. 1. The corresponding DPM is given as follows [4].

$$DPM = \begin{bmatrix} & D\ I\ S\ C\ O & & & \\ cpf_{11} & cpf_{12} & cpf_{13} & cpf_{14} & G \\ cpf_{21} & cpf_{22} & cpf_{23} & cpf_{24} & E \\ cpf_{31} & cpf_{32} & cpf_{33} & cpf_{34} & N \\ cpf_{41} & cpf_{42} & cpf_{43} & cpf_{44} & C\ O \end{bmatrix} \tag{1}$$

where *cpf* represents "Contract Participation Factor" and is like signals that carry information as to which the GENCO has to follow the load demanded by the DISCO. The actual and scheduled steady state power flow through the tie-line are given as;

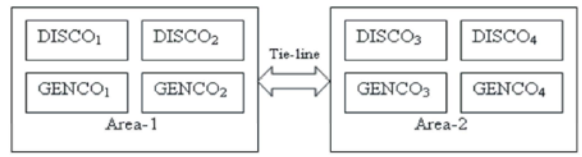

Fig. 1: Schematic diagram of two-area system in restructured environment

$$\Delta P_{tie1-2,\,scheduled} = \sum_{i=1}^{2}\sum_{j=3}^{4} cpf_{ij}\Delta P_{L\,j} - \sum_{i=3}^{4}\sum_{j=1}^{2} cpf_{ij}\Delta P_{L\,j} \tag{2}$$

$$\Delta P_{tie1-2,\,actual} = \left(2\,\pi\,T_{12}/s\right)\left(\Delta F_1 - \Delta F_2\right) \tag{3}$$

And at any given time, the tie-line power error $\Delta P_{tie1-2,error}$ is defined as;

$$\Delta P_{tie1-2,\,error} = \Delta P_{tie1-2,\,actual} - \Delta P_{tie1-2,\,scheduled} \tag{4}$$

The error signal is used to generate the respective ACE signals as in the traditional scenario;

$$ACE_1 = \beta_1 \Delta F_1 + \Delta P_{tie1-2,error} \tag{5}$$

$$ACE_2 = \beta_2 \Delta F_2 + \Delta P_{tie2-1,error} \tag{6}$$

For two area system as shown in Fig. 1, the contracted power supplied by i[th] GENCO is;

$$\Delta Pg_i = \sum_{j=1}^{DISCO=4} cpf_{i\,j}\Delta PL_j \tag{7}$$

Also note that $\Delta PL_{1,LOC} = \Delta PL_1 + \Delta PL_2$ and $\Delta PL_{2,LOC} = \Delta PL_3 + \Delta PL_4$. In the proposed LFC implementation, the contracted load is fed forward through the DPM matrix to GENCO set points. The actual loads affect system dynamics via the input $\Delta PL_{,LOC}$ to the power system blocks. Any mismatch between actual and contracted demands will result in frequency deviations that will drive LFC to re dispatch the GENCOs according to ACE participation factors, i.e., apf_{11}, apf_{12}, apf_{21} and apf_{22}. The state space representation of the minimum realization model of '*N*' area interconnected power system may be expressed as [9].

$$\begin{aligned} \dot{x} &= Ax + Bu + \Gamma d \\ y &= C\,x \end{aligned} \tag{8}$$

where $x = [x_1^T, \Delta p_{ei} \ldots x_{(N-1)}^T, \Delta p_{e(N-1)} \ldots x_N^T]^T$, *n*- state vector

$$n = \sum_{i=1}^{N} n_i + (N-1)$$

$u = [u_1,...u_N]^T = [\Delta P_{C1}...P_{CN}]^T, N$ - Control input vector,

$d = [d_1,...d_N]^T = [\Delta P_{D1}...P_{DN}]^T, N$ - Disturbance input vector

$y = [y_1...y_N]^T, 2N$ - Measurable output vector

where A is system matrix, B is the input distribution matrix, Γ is the disturbance distribution matrix, C is the control output distribution matrix, x is the state vector, u is the control vector and d is the disturbance vector consisting of load changes.

Hydrogen Energy Storage (HES) Systems: Generally the optimization schedule of any distributed energy sources depends on the constraints of the problem which are load limits, actual generation capabilities, status of the battery, forecasted production schedule. Hydrogen energy is one of the promising alternatives that can be used as an energy carrier. The universality of hydrogen implies that it can replace other fuels for stationary generating units for power generation in various industries. So Hydrogen energy is a serious contender for future energy storage due to its versatility and consequently, producing hydrogen from renewable resources using electrolysis is currently the most desirable objective available. Having all the advantages of fossil fuels, hydrogen is free of harmful emissions when used with dosed amount of oxygen, thus reducing the greenhouse effect [13]. Essential elements of a hydrogen energy storage system comprise an electrolyzer unit which converts electrical energy input into hydrogen by decomposing water molecules, the hydrogen storage system itself and a hydrogen energy conversion system which converts the stored chemical energy in the hydrogen back to electrical energy as shown in Fig. 3.

An Aqua Electrolyzer (AE) is a device that produces hydrogen and oxygen from water. Water electrolysis is a reverse process of electrochemical reaction that takes place in a fuel cell. An aqua electrolyzer converts dc electrical energy into chemical energy stored in hydrogen. From electrical circuit point of view, an aqua electrolyzer can be considered as a voltage-sensitive nonlinear dc load. For a given aqua electrolyzer, within its rating range, the higher the dc voltage applied, the larger is the load current. That is, by applying a higher dc voltage, more H_2 can be generated. Aqua Electrolyzer is considered as a subsystem which absorbs the rapidly fluctuating output power. It generates hydrogen and stores in the hydrogen tank and this hydrogen is used as fuel for the fuel cell. The transfer function of AE can be expressed as first order lag:

$$G_{AE}(s) = \frac{K_{AE}}{1 + sT_{AE}} \tag{9}$$

Fuel Cell for Energy Storage with Aqua Electrolyzer: Fuel Cells are static energy conversion device which are considered to be an important resource in hybrid distributed power system due to the advantages like high efficiency, low pollution etc. An electrolyzer uses electrolysis to breakdown water into hydrogen and oxygen. The oxygen is dissipated into the atmosphere and the hydrogen is stored so it can be used for future generation. A fuel cell converts stored chemical energy, in this case hydrogen, directly into electrical energy. A fuel cell consists of two electrodes that are separated by an electrolyte as shown in Fig. 2. Hydrogen is passed over the anode (negative) and oxygen is passed over the cathode (positive) causing hydrogen ions and electrons to form at the anode. The energy produced by the various types of cells depends on the operation temperature, the type of fuel cell and the catalyst used. Fuel cells do not produce any pollutants and have no moving parts.

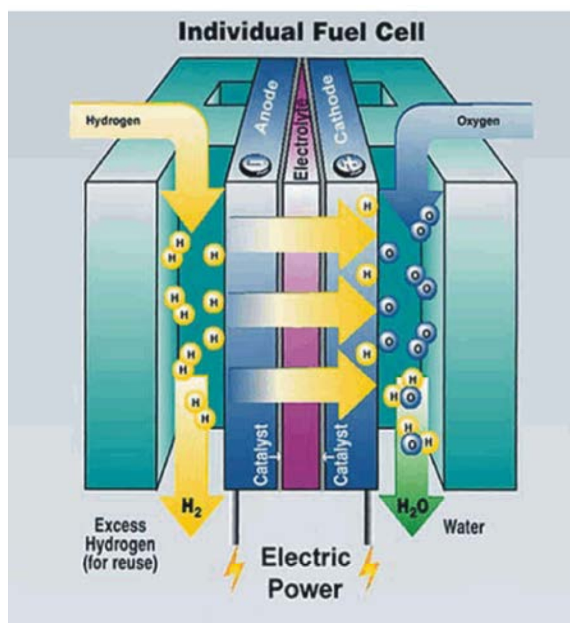

Fig. 2: Structure of a fuel cell

The transfer function of Fuel Cell (FC) can be given by a simple linear equation as;

$$G_{FC}(s) = \frac{K_{FC}}{1+sT_{FC}} \quad (10)$$

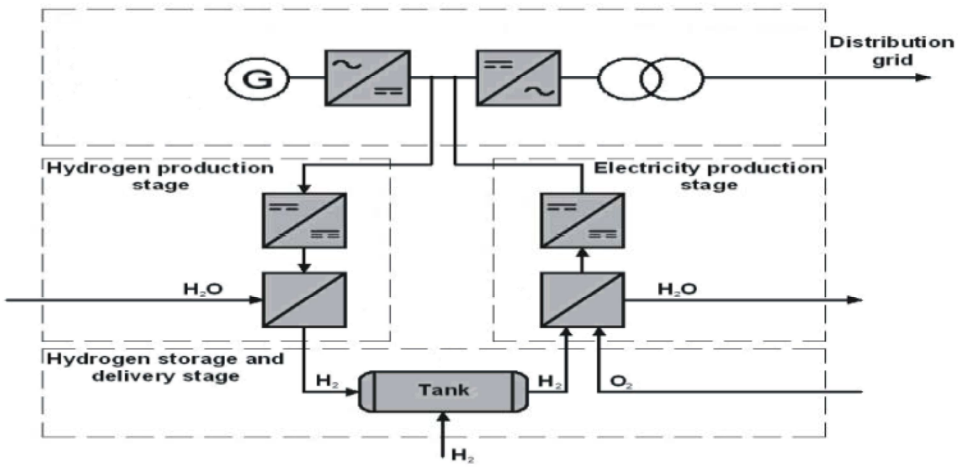

Fig. 3: Block diagram of the hydrogen storage unit

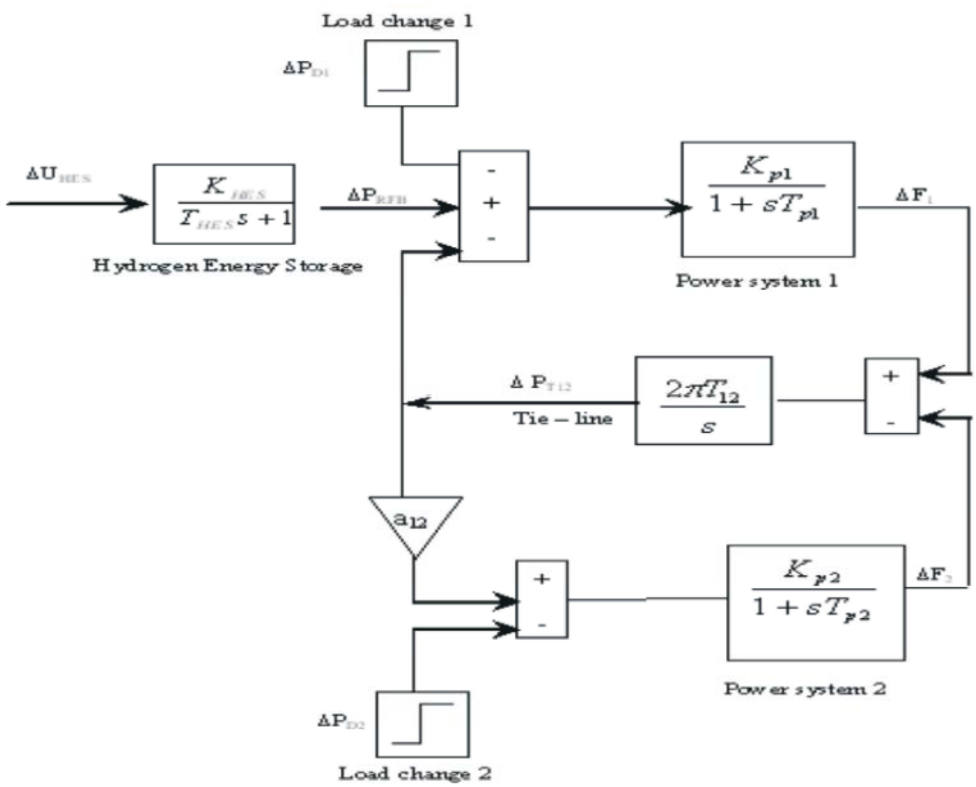

Fig. 4: Linearized reduction model for the control design

The over all transfer function of hydrogen Energy storage unit has can be;

$$G_{HES}(s) = \frac{K_{HES}}{1+sT_{HES}} = \frac{K_{AE}}{1+sT_{AE}} * \frac{K_{FC}}{1+sT_{FC}} \quad (11)$$

Control Design of Hydrogen Energy Storage Unit

The control actions of Hydrogen Energy Storage (HES) units with Fuel Cell (FC) simply referred as HES are found to be superior to the action of the governor system in terms of the response speed against, the frequency fluctuations. The HES units are tuned to suppress the peak value of frequency deviations quickly against the sudden load change, subsequently the governor system are actuated for compensating the steady state error of the frequency deviations. Fig. 4 shows the linearized reduction model for the control design of two area interconnected power system with HES units. The HES unit is modeled as an active power source to area 1 with a time constant T_{HES} and gain constant K_{HES}. Assuming the time constants T_{HES} is regarded as 0 sec for the control design [9], then the state equation of the system represented by Fig. 4 becomes;

$$\begin{bmatrix} \Delta\dot{F}_1 \\ \Delta\dot{P}_{T12} \\ \Delta\dot{F}_2 \end{bmatrix} = \begin{bmatrix} -\frac{1}{T_{p1}} & -\frac{K_{p1}}{T_{p1}} & 0 \\ 2\pi T_{12} & 0 & -2\pi T_{12} \\ 0 & \frac{a_{12}\,k_{p2}}{T_{p2}} & -\frac{1}{T_{p2}} \end{bmatrix} \begin{bmatrix} \Delta F_1 \\ \Delta P_{T12} \\ \Delta F_2 \end{bmatrix} + \begin{bmatrix} \frac{k_{p1}}{T_{p1}} \\ 0 \\ 0 \end{bmatrix} [\Delta P_{HES}] \tag{12}$$

The design process starts from the reduction of two area system into one area which represents the Inertia centre mode of the overall system. The controller of HES is designed for the equivalent one area system to reduce the frequency deviation of inertia centre. The equivalent system is derived by assuming the synchronizing coefficient T_{12} to be large. From the state equation of $\Delta\dot{P}_{T12}$ in Eq. (12).

$$\frac{\Delta\dot{P}_{T12}}{2\pi T_{12}} = \Delta F_1 - \Delta F_2 \tag{13}$$

Setting the value of T_{12} in Eq. (13) to be infinity yields $\Delta F_1 = \Delta F_2$. Next, by multiplying state equation of $\Delta\dot{F}_1$ *and* $\Delta\dot{F}_2$ by $\frac{T_{p1}}{k_{p1}}$ and $\frac{T_{p2}}{a_{12}\,k_{p2}}$ respectively, then;

$$\frac{T_{p1}}{k_{p1}}\Delta\dot{F}_1 = -\frac{1}{k_{p1}}\Delta F_1 - \Delta P_{T12} + \Delta P_{HES} \tag{14}$$

$$\frac{T_{p2}}{a_{12}\,k_{p2}}\Delta\dot{F}_2 = \frac{-1}{k_{p2}\,a_{12}}\Delta F_2 + \Delta P_{T12} \tag{15}$$

By summing Eq. (14) and Eq. (15) and using the above relation $\Delta F_1 = \Delta F_2 = \Delta F$.

$$\Delta\dot{F} = \frac{\left(-\frac{1}{k_{p1}} - \frac{1}{k_{p2}a_{12}}\right)}{\left(\frac{T_{p1}}{k_{p1}} + \frac{T_{p2}}{k_{p2}a_{12}}\right)}\Delta F + \frac{1}{\left(\frac{T_{p1}}{k_{p1}} + \frac{T_{p2}}{k_{p2}a_{12}}\right)}\Delta P_{HES} + C\Delta P_D \tag{16}$$

where ΔP_D is the load change in this system and the control $\Delta P_{HES} = -K_{HES}\,\Delta F$ is applied then.

$$\Delta F = \frac{C}{s + A + K_{HES}\,B}\Delta P_D \tag{17}$$

where $A = \left(-\frac{1}{k_{p1}} - \frac{1}{k_{p2}a_{12}}\right) \Big/ \left(\frac{T_{p1}}{k_{p1}} + \frac{T_{p2}}{k_{p2}a_{12}}\right)$,

$$B = \frac{1}{\left[\frac{T_{p1}}{K_{p1}} + \frac{T_{p2}}{K_{p2}a_{12}}\right]}$$

where C is the proportionality constant between change in frequency and change in load demand. Since the control action of HES unit is to suppress the deviation of the frequency quickly against the sudden change of ΔP_D, the percent reduction of the final value after applying a step change ΔP_D can be given as a control specification. In Eq (17) the final values with $K_{HES} = 0$ and with $K_{HES} \neq 0$ are C/A and C/(A+K_{HES} B) respectively therefore the percentage reduction is represented by;

$$C/(A+K_{HES}\,B) \big/ (C/A) = R/100 \tag{18}$$

For a given R, the control gain of HES is calculated as;

$$K_{HES} = \frac{A}{BR}(100 - R) \tag{19}$$

The linearized model of an interconnected two-area reheat thermal power system in deregulated environment is shown in Fig. 5 after incorporating HES unit with FC.

Design of Decentralized PI and PI+ Controllers

Design and Implementation of PI Controller: The proportional and Integral controller gain values (K_{pi}, K_{Ii}) are tuned based on the settling time of the output response of the system (especially the frequency deviation) using Bacterial Foraging Optimization (BFO) technique. The closed loop stability of the system with decentralized PI controllers is assessed using settling time of the system output response. It is observed that the system whose output response settles fast will have minimum settling time based criterion [16] and can be expressed as;

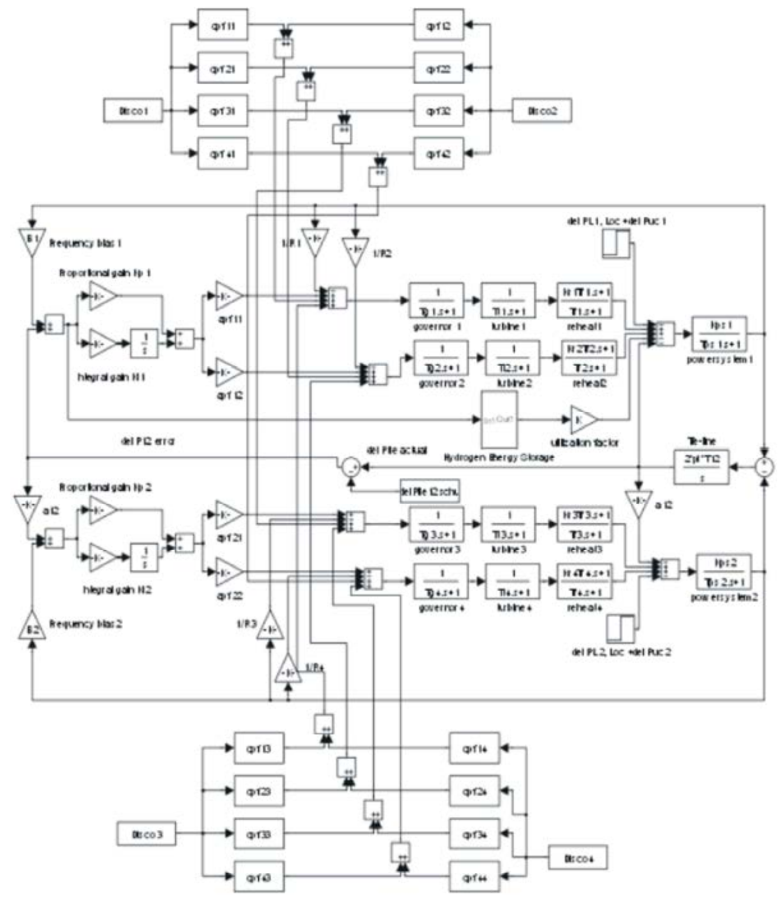

Fig. 5: Simulink model of a Two- Area Thermal Reheat Interconnected Power System (TATRIPS) in restructured environment with Hydrogen Energy Storage unit and Fuel Cell.

$$F\,(K_p\,,K_i\,) = \min\ (\,\zeta_{si})\tag{20}$$

$$U_1\ = -K_p\ ACE_1\ - K_I \int ACE_1\ \ dt\tag{21}$$

$$U_2\ = -K_p\ ACE_2\ - K_I \int ACE_2\ \ dt\tag{22}$$

where K_P is the Proportional gain, K_I is the Integral gain, *ACE* is the Area Control Error, U_1, U_2 are the Control input requirement of the respective areas, ζ_{si} is the settling time of the frequency deviation of the ith area under disturbance. The relative simplicity of this controller is a successful approach towards the zero steady state error in the frequency of the system. With these optimized gain values the performance of the system is analyzed and various PSRAI are computed.

Design and Implementation of PI$^+$ Controller: In practice, LFC systems use proportional-integral (PI) controllers that are designed using a linear model. These controllers are incapable to gain good dynamical performance for a wide range of operating conditions especially in deregulated environments. In PI controller K_P provides stability and high frequency response and K_I ensures that the average error is driven to zero. So no long term error, as the two gains are tuned. This normally provides high responsive systems. But the predominant weakness of PI controller is it often produces excessive overshoot to a step command [16]. The PI controller lacks a windup function to control the integral value during saturation. But PI$^+$ uses a low pass filter on the command signal to limit the overshoot. The Proportional and Integral plus (PI$^+$) controller as the name indicates is an enhancement to PI. Because of the overshoot, the integral gain in PI controllers is limited in magnitude. PI$^+$ control uses a low-pass filter on the command signal to remove overshoot. In this way, the integral gain can be raised to higher values. PI$^+$ is useful in applications. The primary shortcoming of PI$^+$ is that the command filter also reduces the controller's command response [17].

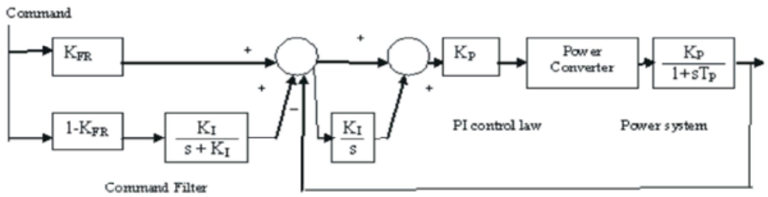

Fig. 6: Block diagram for PI^+ control

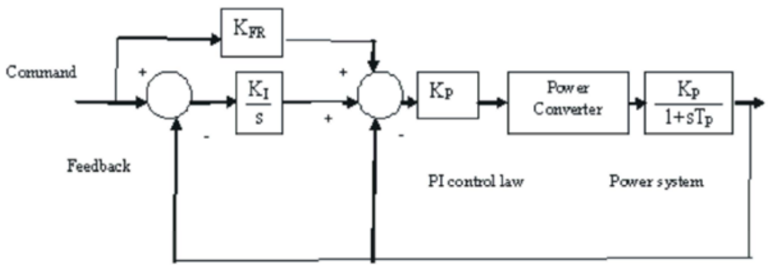

Fig. 7: Pseudo Derivative Feedback with Feed forward (PDFF) controller

The PI^+ controller is shown in Fig. 6. The system is the PI controller with a command filter added. The degree to which a PI^+ controller filters the command signal is determined by the gain K_{FR}. When K_{FR} is 1, all filtering is removed and the controller is identical to a PI controller. Filtering is most severe when K_{FR} is zero. When K_{FR} is zero, command is filtered by $K_I/(s + K_I)$, which is a single-pole low-pass filter at the frequency K_I(in rad/sec). This case will allow the highest integral gain but also will most severely limit the controller command response. Typically, $K_{FR} = 0$ will allow an increase of almost three times in the integral gain but will reduce the bandwidth by about one-half when compared with $K_{FR} = 1$ (PI control). Finding the optimal value of K_{FR} depends on the application, but a value of 0.65 has been found to work in many applications. This value typically allows the integral gain to more than double while reducing the bandwidth by only 15%-20% [17]. K_I as the frequency of the command low-pass filter because it is excellent at canceling the peaking caused by the integral gain. PI^+ control is that it uses the command filter to attenuate the peaking caused by PI. The peaking caused by K_I can be cancelled by the attenuation of a low-pass filter with a break of K_I.

In Fig. 6 the control law for PI^+ controller is represented as;

$$Control = K_P\left(command\left(K_{FR} + (1 - K_{FR})\frac{K_I}{s + K_I}\right) - Feedback\right)\left(1 + \frac{K_I}{s}\right) \tag{22}$$

In PI^+ is often referred as Pseudo Derivative Feedback with Feed forward (PDFF) is shown in Fig7 and the control law for PI^+ controller is represented as;

$$Control = K_P\left((command - Feedback)\frac{K_I}{s} + K_{FR}\,command - Feedback\right) \tag{23}$$

PDFF is an alternative way to implement PI^+; it is useful in digital systems because there are no multiplications before the integral. Multiplication, when not carefully constructed, causes numerical noise. That noise prior to the integrator may cause drift in the control loop as the round-off error accumulates in the integrator. PDFF has a single operation, a subtraction, which is usually noiseless, before the integration and thus easily avoids such noise.

Bacterial Foraging Optimization (BFO) Technique: BFO method was introduced by Passino [18] motivated by the natural selection which tends to eliminate the animals with poor foraging strategies and favour those having successful foraging strategies. The foraging strategy is governed by four processes namely Chemotaxis, Swarming, Reproduction and Elimination and Dispersal. Chemotaxis process is the characteristics of movement of bacteria in search of food and consists of two processes namely swimming and tumbling. A bacterium is said to be swimming if it moves in a predefined direction and tumbling if it starts moving in an altogether different direction. To represent a tumble, a unit length random direction $\phi(j)$ is generated. Let, "j" is the index of chemotactic step, "k" is reproduction step and "l" is the elimination dispersal event. $\theta_i(j,k,l)$, is the position of i^{th} bacteria at j^{th} chemotactic step k^{th} reproduction step and l^{th} elimination dispersal event. The position of the bacteria in the next chemotactic step after a tumble is given by;

$$\theta^i(j+1, \quad k, \quad l) = \theta^i(j, \quad k, \quad l) + C(i)\,\phi(j) \tag{24}$$

If the health of the bacteria improves after the tumble, the bacteria will continue to swim to the same direction for the specified steps or until the health degrades. Bacteria exhibits swarm behavior i.e. healthy bacteria try to attract other bacterium so that together they reach the desired location (solution point) more rapidly. The effect of swarming is to make the bacteria congregate into groups and moves as concentric patterns with high bacterial density [16]. Mathematically swarming behavior can be modeled.

$$\begin{aligned} J_{cc}\left(\theta, P(j,k,l)\right) &= \sum_{i=1}^{S} J^i cc\left(\theta, \theta^i(j.k.l)\right) \\ &= \sum_{i=1}^{S}\left[-d_{attract}\exp\left(-\omega_{attract}\right)\sum_{m=1}^{p}\left(\theta^m - \theta_m^i\right)^2\right] \\ &+ \sum_{i=1}^{S}\left[-h_{repelent}\exp\left(-w_{repelent}\right)\sum_{m=1}^{p}\left(\theta^m - \theta_m^i\right)^2\right] \end{aligned} \tag{25}$$

J_{CC} is the relative distance of each bacterium from the fittest bacterium, S is the number of bacteria, p is the number of parameters to be optimized, θ^n is the position of the fittest bacteria, $d_{attract}$, $\omega_{attract}$, $h_{repelent}$, $\omega_{repelent}$ are the different co-efficients representing the swarming behaviour of the bacteria which are to be chosen properly. In Reproduction step, population members who have sufficient nutrients will reproduce and the least healthy bacteria will die. The healthier population replaces unhealthy bacteria which get eliminated owing to their poorer foraging abilities. This makes the population of bacteria constant in the evolution process. In this process a sudden unforeseen event may drastically alter the evolution and may cause the elimination and / or dispersion to a new environment. Elimination and dispersal helps in reducing the behavior of stagnation i.e., being trapped in a premature solution point or local optima. The flowchart of BFO algorithm is shown in Fig.8.

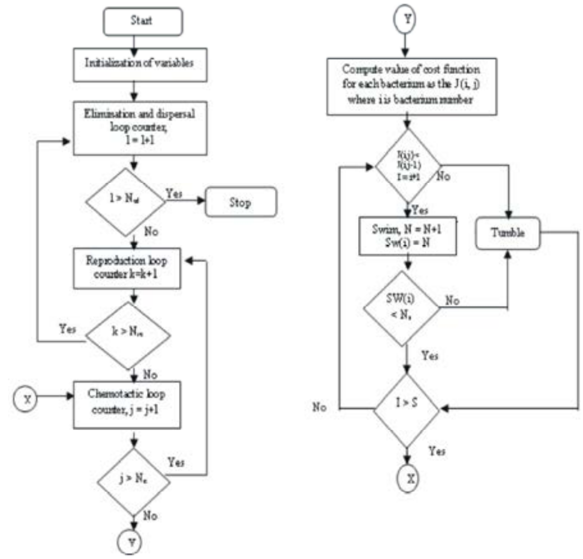

Fig. 8: Flowchart for BFO algorithm

Computation of Power System Ancillary Service Requirement Assessment Indices: The Power System Ancillary Service Requirement Assessment Indices (PSASRAI) namely, Feasible Assessment Indices (FAI) i.e., when the system is under normal operating condition with both units in operation and Comprehensive Assessment Indices (CAI) i.e., when the system's are one or more units are outage in any area are obtained considering the $GENCO_4$ in area 2 is outage are considered in this study. From these Assessment Indices indicates the restorative measures like the magnitude of control input requirement, rate of change of control input requirement can be adjudged.

Feasible Restoration Indices

Scenario 1: Poolco based transaction

The optimal Proportional and Integral plus (PI^+) controller gains are obtained for TATIPS considering various case studies for framing the Feasible Assessment Indices (FAI) which were obtained based on Area Control Error (ACE) as follows:

Case 1: In the TATRIPS considering both areas have two thermal reheat units. For Poolco based transaction, consider a case where the GENCOs in each area participate equally in LFC. For Poolco based transaction: the load change occurs only in area 1. It denotes that the load is demanded only by DISCO 1 and DISCO 2. Let the value of this load demand be 0.1 p.u MW for each of them i.e. ΔPL_1= 0.1 p.u MW, ΔPL_2= 0.1 p.u MW, $\Delta PL_3 = \Delta PL_4$= 0.0. DISCO Participation Matrix (DPM) referring to Eq. (1) is considered as [4].

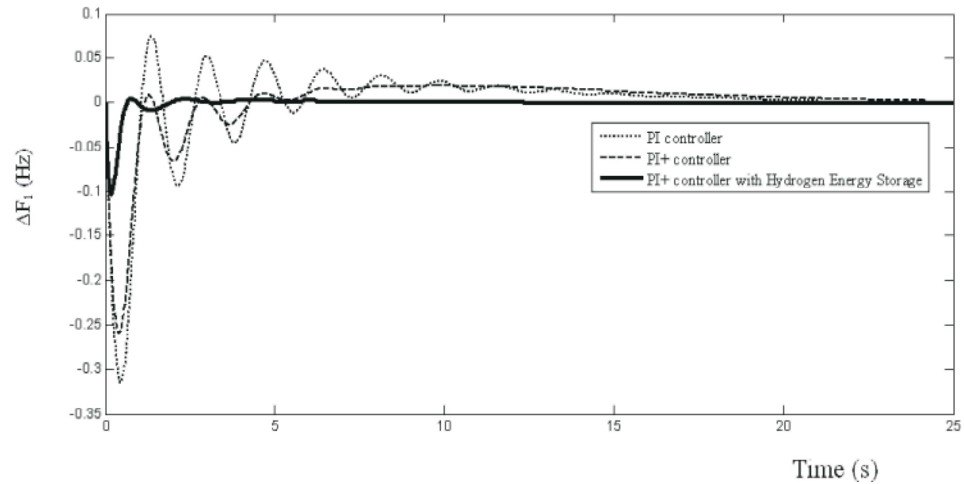

Fig. 9(a): ΔF_1 (Hz) Vs Time (s)

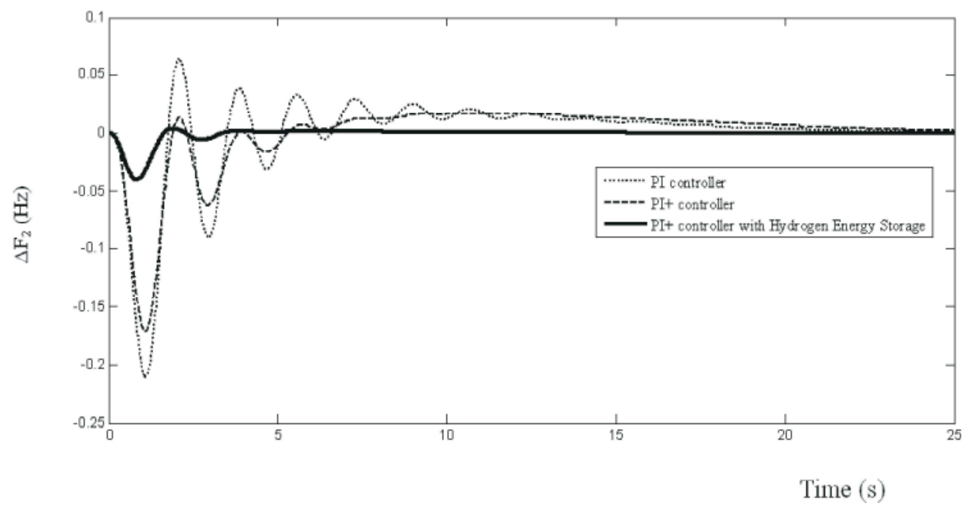

Fig. 9(b): ΔF_2 (Hz) Vs Time (s)

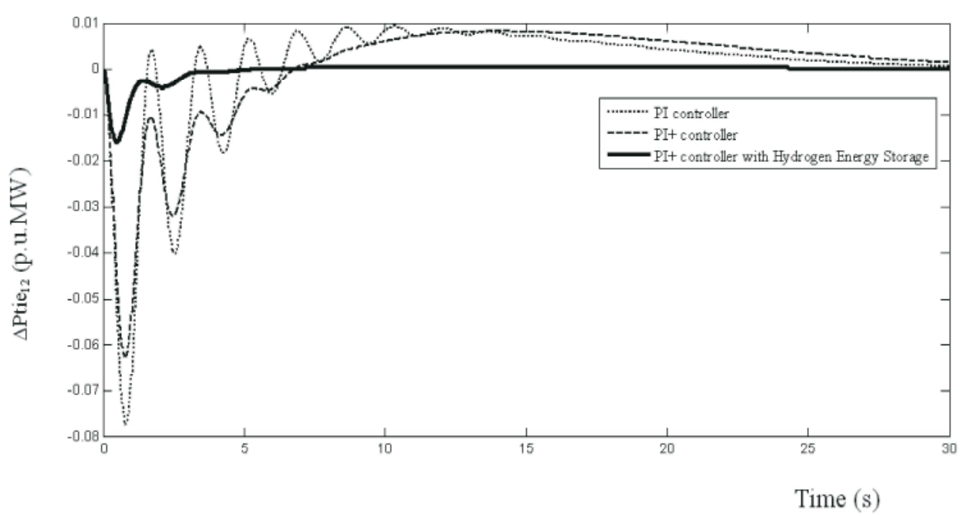

Fig. 9(c): $\Delta Ptie_{12}$ (p.u.MW) Vs Time (s)

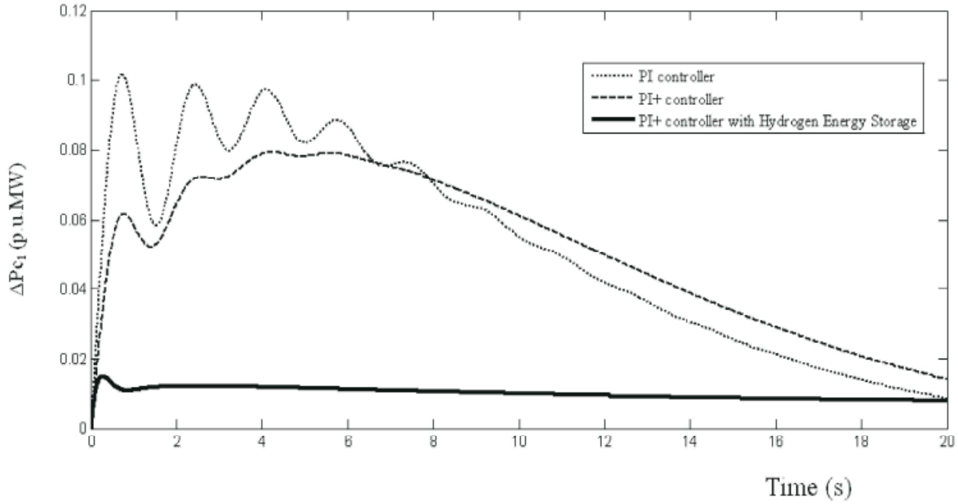

Fig. 9(d): ΔPc_1 (p.u.MW) Vs Time (s)

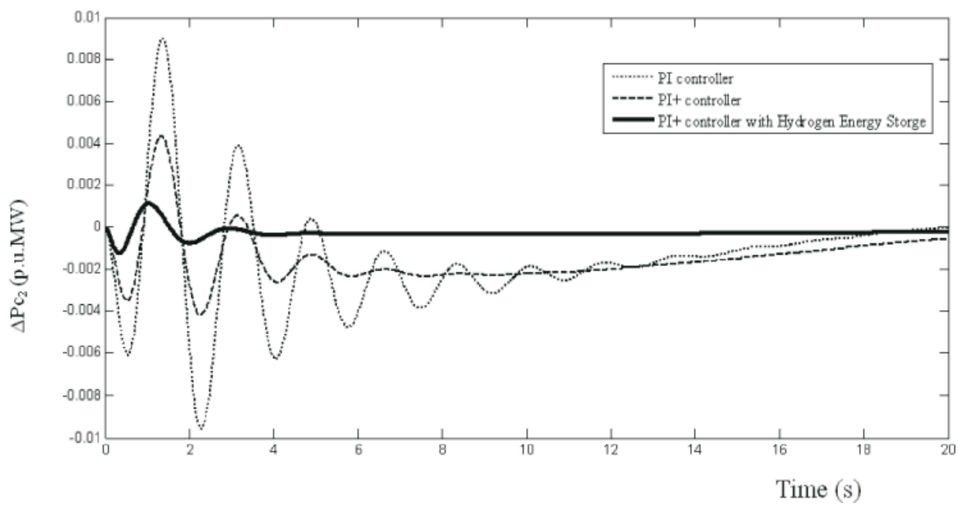

Fig. 9(e): ΔPc_2 (p.u.MW) Vs Time (s)

Fig. 9: Dynamic responses of the frequency deviations, tie- line power deviations and Control input deviations for TATRIPS in the restructured scenario-1 (poolco based transactions) using PI^+ controller

$$DPM = \begin{bmatrix} 0.5 & 0.5 & 0 & 0 \\ 0.5 & 0.5 & 0 & 0 \\ 0 & 0 & 0 & 0 \\ 0 & 0 & 0 & 0 \end{bmatrix} \quad (26)$$

Note that DISCO 3 and DISCO 4 do not demand power from any of the GENCOs and hence the corresponding contract participation factors (columns 3 and 4) are zero. DISCO 1 and DISCO 2 demand identically from their local GENCOs, viz., GENCO 1 and GENCO 2. Therefore, $cpf_{11} = cpf_{12} = 0.5$ and $cpf_{21} = cpf_{22} = 0.5$. The frequency deviations (ΔF) of both-area, tie-line power deviation (ΔP_{tie}) and control input requirements deviations (ΔP_c) of both areas are as shown the Fig. 9. The settling time (ς_s) and peak over /under shoot (Mp) of the control input deviations (ΔP_c) in both the area were obtained from Fig. 9. From the Fig. 9 (d) and (e) the corresponding Feasible Assessment Indices FAI_1, FAI_2, FAI_3 and FAI_4 are calculated as follows;

Step 6.1: The Feasible Assessment Index 1 (ε_1) is obtained from the ratio between the settling time of the control input deviation $\Delta P_{c1}(\varsigma_{s1})$ response of area 1 and power system time constant (T_{p1}) of area 1.

$$FRI_1 = \frac{\Delta P_{c1}(\varsigma_{s1})}{T_{p1}} \tag{27}$$

Step 6.2: The Feasible Assessment Index 2 (ε_2) is obtained from the ratio between the settling time of the control input deviation $\Delta P_{c2}(\varsigma_{s2})$ response of area 2 and power system time constant (T_{p2}) of area 2

$$FRI_2 = \frac{\Delta P_{c2}(\varsigma_{s2})}{T_{p2}} \tag{28}$$

Step 6.3: The Feasible Assessment Index 3 (ε_3) is obtained from the peak value of the control input deviation $\Delta P_{c1}(\varsigma_p)$ response of area 1 with respect to the final value $\Delta P_{c1}(\varsigma_s)$.

$$FRI_3 = \Delta P_{c1}(\varsigma_p) - \Delta P_{c1}(\varsigma_s) \tag{29}$$

Step 6.4: The Feasible Assessment Index 4 (ε_4) is obtained from the peak value of the control input deviation $\Delta P_{c2}(\varsigma_p)$ response of area 1 with respect to the final value $\Delta P_{c2}(\varsigma_s)$

$$FRI_4 = \Delta P_{c2}(\varsigma_p) - \Delta P_{c2}(\varsigma_s) \tag{30}$$

Case 2: This case is also referred a Poolco based transaction on TATRIPS where in the GENCOs in each area participate not equally in LFC and load demand is more than the GENCO in area 1 and the load demand change occurs only in area 1. This condition is indicated in the column entries of the DPM matrix and sum of the column entries is more than unity.

Case 3: It may happen that a DISCO violates a contract by demanding more power than that specified in the contract and this excess power is not contracted to any of the GENCOs. This uncontracted power must be supplied by the GENCOs in the same area to $_4$the DISCO. It is represented as a local load of the area but not as the contract demand. Consider scenario-1 again with a modification that $DISCO_1$ demands 0.1 p.u MW of excess power i.e., $\Delta Puc_{,1}$= 0.1 p.u MW and $\Delta Puc_{,2}$ = 0.0 p.u MW. The total load in area 1 = Load of $DISCO_1$ + Load of $DISCO_2$ = $\Delta PL_1 + \Delta Puc_1 + \Delta PL_2$=0.1+0.1+0.1=0.3 p.u MW.

Case 4: This case is similar to Case 2 to with a modification that $DISCO_3$ demands 0.1 p.u.MW of excess power i.e., ΔPuc_2 = 0.1 p.u MW and., ΔPuc_1 = 0 p.u MW. The total load in area 2 = Load of $DISCO_3$ + Load of $DISCO_4 = \Delta PL_1 + \Delta PL_2 + \Delta Puc_2$ = 0+0+0.1 = 0.1 p.u MW.

Case 5: In this case which is similar to Case 2 with a modification that $DISCO_1$ and $DISCO_3$ demands 0.1p.u.MW of excess power i.e., ΔPuc_1 = 0.1p.u.MW and ΔPuc_2 = 0.1p.u.MW. The total load in area 1 = Load of $DISCO_1$ +Load of $DISCO_2$ = $\Delta PL_1 + \Delta Puc_1 + \Delta PL_2$ = 0.1+0.1+0.1 = 0.3 p.u MW and total demand in area 2 = Load of $DISCO_3$ +Load of $DISCO_4 = \Delta PL_3 + \Delta Puc_2 + \Delta PL_4$ = 0+0.1+0 = 0.1 p.u MW.

6.1.2 Scenario 2: Bilateral Transaction

Case 6: Here all the DISCOs have contract with the GENCOs and the following DISCO Participation Matrix (DPM) be considered [4].

$$DPM = \begin{bmatrix} 0.4 & 0.25 & 0.2 & 0.4 \\ 0.3 & 0.15 & 0.1 & 0.2 \\ 0.1 & 0.4 & 0.3 & 0.25 \\ 0.2 & 0.2 & 0.4 & 0.15 \end{bmatrix} \tag{31}$$

In this case, the $DISCO_1$, $DISCO_2$, $DISCO_3$ and $DISCO_4$, demands 0.15 p.u MW, 0.05 p.u MW, 0.15 p.u MW and 0.05 p.u MW from GENCOs as defined by *cpf* in the DPM matrix and each GENCO participates in LFC as defined by the following ACE participation factor apf_{11} = apf_{12} = 0.5 and apf_{21} = apf_{22} = 0.5. The dynamic responses are shown in Fig. 10. From this Fig. 10 the corresponding FAI_1, FAI_2, FAI_3 and FAI_4 is calculated.

Case 7: For this case also bilateral transaction on TATRIPS is considered with a modification that the GENCOs in each area participate not equally in LFC and load demand is more than the GENCO in both the areas. But it is assumed that the load demand change occurs in both areas and the sum of the column entries of the DPM matrix is more than unity.

Case 8: Considering in the case 7 again with a modification that DISCO 1 demands 0.1 p.u MW of excess power i.e., ΔPuc_1= 0.1 p.u.MW and ΔPuc_2 = 0.0 p.u MW. The total load in area 1 = Load of $DISCO_1$ +Load of $DISCO_2 = \Delta PL_1 + \Delta Puc_1 + \Delta PL_2$ =0.15+0.1+0.05 =0.3 p.u MW and total load in area 2 = Load of $DISCO_3$ +Load of $DISCO_4 = \Delta PL_3 + \Delta PL_4$=0.15+0.05 =0.2 p.u MW.

Case 9: In the case which similar to case 7 with a modification that $DISCO_3$ demands 0.1 p.u.MW of excess power i.e., $\Delta Puc_{,2}$ = 0.1 p.u MW. The total load in area 1 = Load of $DISCO_1$ +Load of $DISCO_2 = \Delta PL_3 + \Delta PL_4$ = 0.15+0.05 =0.2 p.u.MW and total demand in area 2 = Load of $DISCO_3$ +Load of $DISC_4 = \Delta PL_3 + \Delta PL_4 + \Delta Puc_3$ = 0.15+0.05+0.1 = 0.3 p.u MW.

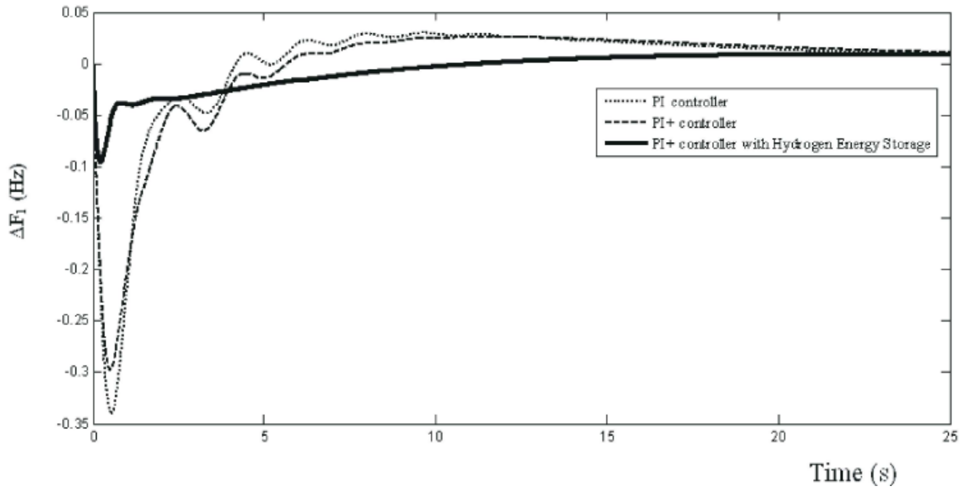

Fig. 10(a): ΔF_1 (Hz) Vs Time (s)

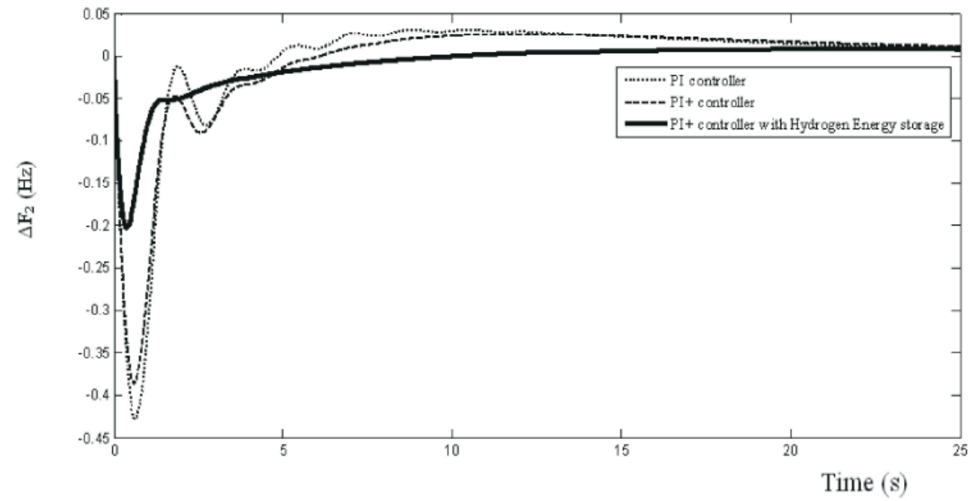

Fig. 10(b): ΔF_2 (Hz) Vs Time (s)

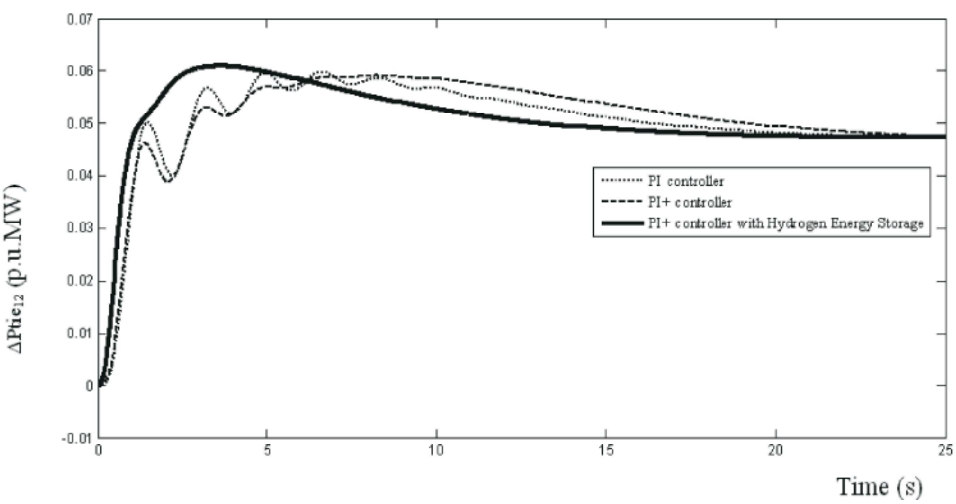

Fig. 10(c): $\Delta Ptie_{12,\ actual}$ (p.u.MW) Vs Time (s)

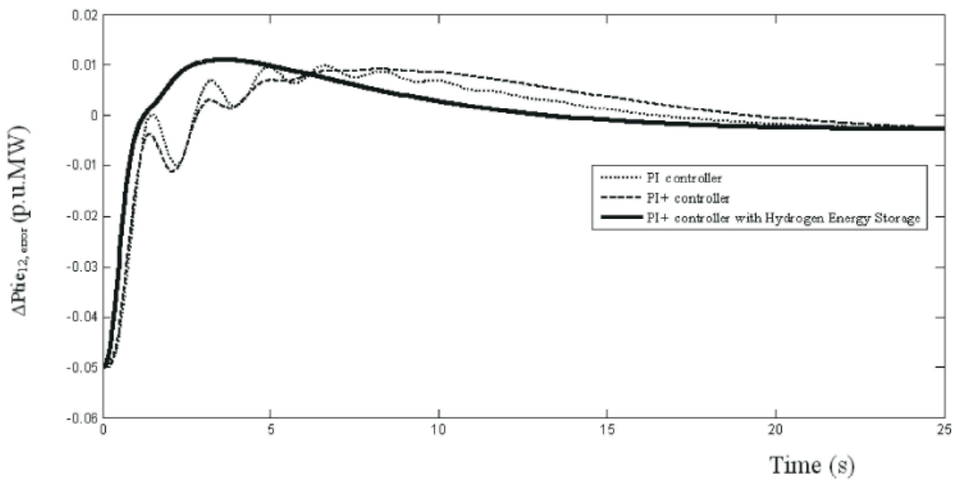

Fig. 10(d): $\Delta Ptie_{12,\,error}$ (p.u.MW) Vs Time (s)

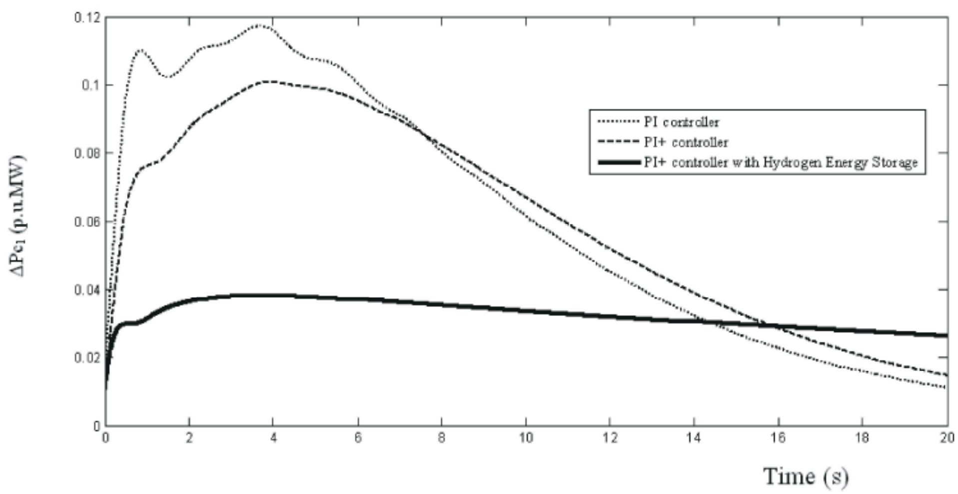

Fig. 10(e): ΔPc_1 (p.u.MW) Vs Time (s)

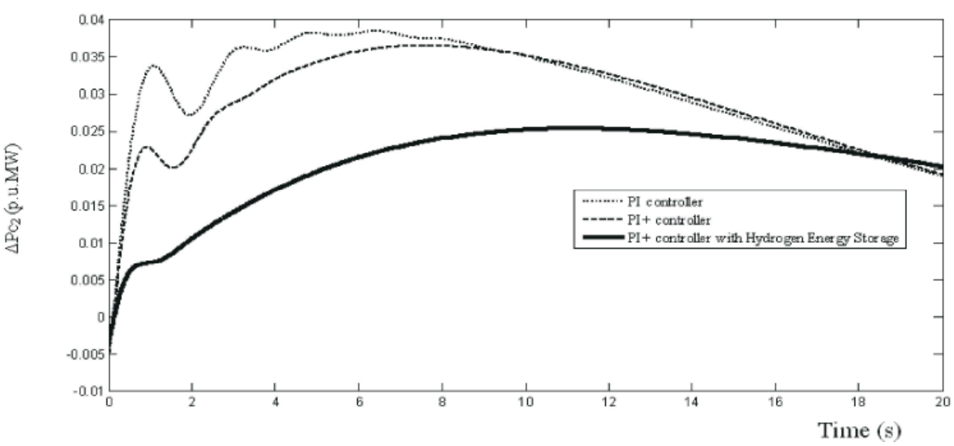

Fig. 10(f): ΔPc_2 (p.u.MW) Vs Time (s)

Fig. 10: Dynamic responses of the frequency deviations, tie- line power deviations and Control input deviations for TATRIPS in the restructured scenario-2 (bilateral based transactions) using PI^+ controller

Case 10: In the case which similar to case 7 with a modification that $DISCO_1$ and $DISCO_3$ demands 0.1 p.u MW of excess power i.e., $\Delta Puc_{,1}$= 0.1 p.u MW and $\Delta Puc_{,2}$ = 0.1 p.u MW. The total load in area 1 = Load of $DISCO_1$ + Load of $DISCO_2$ = $\Delta PL_1 + \Delta Puc_1 + \Delta PL_2$ = 0.15+0.1+0.05 = 0.3 p.u MW and total load in area 2 = Load of $DISCO_3$ + Load of $DISCO_4$ = $\Delta PL_3 + \Delta Puc_3 + \Delta PL_4$ = 0.15+0.1+0.05 = 0.3 p.u MW.

For the Cases 1-10, Feasible Assessment Indices (FAI_1, FAI_2, FAI_3 and FAI_4) or ε_1, ε_2, ε_3 and ε_4 are calculated using (27 to 30) are tabulated in Table 4.

Comprehensive Assessment Indices: Apart from the normal operating condition of the TATRIPS few other case studies like one unit outage in an area, outage of one distributed generation in an area are considered individually. With the various case studies and based on their optimal gains the corresponding CAI is obtained as follows.

Case 11: In the TATRIPS considering all the DISCOs have contract with the GENCOs but GENCO4 is outage in area-2. In this case, the $DISCO_1$, $DISCO_2$, $DISCO_3$ and $DISCO_4$ demands 0.15 p.u MW, 0.05 p.u MW, 0.15 pu. MW and 0.05 pu.MW from GENCOs as defined by *cpf* in the DPM matrix (26). The output $GENCO_4$ = 0.0 p.u MW.

Case 12: Consider in this case which is same as Case 11 but DISCO 1 demands 0.1 p.u.MW of excess power i.e., ΔPuc_1= 0.1 p.u.MW and ΔPuc_2 = 0.0 p.u MW. The total load in area 1 = Load of $DISCO_1$ + Load of $DISCO_2$ = $\Delta PL_1 + \Delta Puc_1 + \Delta PL_2$= 0.15+0.1+0.05 = 0.3 p.u MW and total load in area 2 = Load of $DISCO_3$ + Load of $DISCO_4$ = $\Delta PL_3 + \Delta PL_4$ =0.15+0.05 =0.2 p.u MW.

Case 13: This case is same as Case 11 with a modification that $DISCO_3$ demands 0.1 p.u MW of excess power i.e., ΔPuc_3 = 0.1 p.u MW. The total load in area 1 = Load of $DISCO_1$ +Load of $DISCO_2$ = $\Delta PL_3 + \Delta PL_4$ =0.15+0.05 =0.2 p.u MW and total demand in area 2 = Load of $DISCO_3$ + Load of $DISCO_4$ = $\Delta PL_3 + \Delta PL_4 + \Delta Puc_3$ =0.15+0.05+0.1 = 0.3 p.u MW.

Case 14: In this case which is similar to Case 11 with a modification that $DISCO_1$ and $DISCO_3$ demands 0.1 p.u MW of excess power i.e., ΔPuc_1= 0.1 p.u.MW and ΔPuc_3 = 0.1 p.u MW. The total load in area 1 = Load of $DISCO_1$ +Load of $DISCO_2$ = $\Delta PL_1 + \Delta Puc_1 + \Delta PL_2$ = 0.15+0.1+0.05 = 0.3 p.u MW and total load in area 2 = Load of $DISCO_3$ + Load of $DISCO_4$ = $\Delta PL_3 + \Delta Puc_3 + \Delta PL_4$ =0.15+0.1+0.05 = 0.3 p.u MW. For the Case 11-14, the corresponding Assessment Indices are referred as Comprehensive Assessment Indices (CAI_1, CAI_2, CAI_3 and CAI_4) are obtained using Eq. (27 to 30) as ε_5, ε_6, ε_7 and ε_8 and $\int P$ is the ancillary service requirement for various case studies are tabulated in Table 5.

Simulation Results and Observations: The Two-Area Thermal Reheat Interconnected Restructured Power System considered for the study consists of two GENCOs and two DISCOs in each area. The nominal parameters are given in Appendix. The optimal solution for the objective function (25) is obtained using the frequency deviations of control areas and tie- line power changes. The gain values of HES with fuel cell (K_{HES}) are calculated using Eq (19) for the given value of speed regulation coefficient (R). The gain value is of the HES with fuel cell is found to be K_{RFB} = 0.67. The PI^+ controller gains (K_p, K_i) are tuned with BFO algorithm by optimizing the solutions of control

Table 1: Optimized Controller parameters of the TATRIPS using PI^+ controller

	Controller gain of AREA 1 With K_{FR} =0.65		Controller gain of AREA 2 With K_{FR} =0.65	
Tatrips	K_{p1}	K_{i1}	K_{p2}	K_{i2}
Case 1	0.341	0.519	0.191	0.105
Case 2	0.384	0.412	0.212	0.125
Case 3	0.428	0.485	0.236	0.133
Case 4	0.396	0.459	0.242	0.142
Case 5	0.412	0.486	0.253	0.146
Case 6	0.316	0.543	0.121	0.209
Case 7	0.336	0.585	0.139	0.201
Case 8	0.341	0.595	0.218	0.192
Case 9	0.357	0.593	0.247	0.258
Case 10	0.364	0.632	0.274	0.242
Case 11	0.384	0.623	0.277	0.198
Case 12	0.401	0.674	0.279	0.236
Case 13	0.419	0.687	0.286	0.253
Case 14	0.462	0.693	0.296	0.258

Table 2: Optimized Controller parameters of the TATRIPS with HES unit using PI^+ controller

Tatrips with HES unit	Controller gain of AREA 1 With K_{FR} =0.65		Controller gain of AREA 2 With K_{FR} =0.65	
	K_{p1}	K_{i1}	K_{p2}	K_{i2}
Case 1	0.228	0.496	0.102	0.124
Case 2	0.252	0.512	0.127	0.131
Case 3	0.287	0.545	0.134	0.145
Case 4	0.296	0.562	0.142	0.213
Case 5	0.328	0.575	0.154	0.236
Case 6	0.241	0.696	0.138	0.296
Case 7	0.283	0.702	0.148	0.334
Case 8	0.378	0.764	0.152	0.386
Case 9	0.398	0.791	0.165	0.375
Case 10	0.402	0.798	0.223	0.381
Case 11	0.427	0.856	0.286	0.393
Case 12	0.494	0.886	0.264	0.396
Case 13	0.538	0.825	0.271	0.462
Case 14	0.591	0.846	0.288	0.476

Table 3: Comparison of the system dynamic performance for TATRIPS

TATRIPS (Poolco based transaction)	Setting time (τ_s) in sec			Peak over / under shoot		
	ΔF_1	ΔF_2	ΔP_{tie}	ΔF_1 in Hz	ΔF_2 in Hz	ΔP_{tie} in p.u MW
PI controller	18.14	17.52	20.13	0.321	0.215	0.082
PI^+ controller	13.21	15.19	17.53	0.253	0.171	0.062
PI^+ controller with HES unit	2.447	2.912	5.135	0.097	0.036	0.015

Table 4(a): Feasible Assessment Indices (FAI) without and with HES unit (utilization factor K=1) for TATRIPS using PI^+ controller

Tatrips	Feasible Assessment Indices (FAI) based on control input deviations (ΔP_c) without HES unit (utilization factor K=0)					Feasible Assessment Indices (FAI) based on control input deviations (ΔP_c) with HES unit (utilization factor K=1)				
	ε_1	ε_2	ε_3	ε_4	$\int P_{C1}$	ε_1	ε_2	ε_3	ε_4	$\int P_{HES}$
Case 1	0.912	0.856	0.123	0.014	1.011	0.801	0.704	0.082	0.006	0.534
Case 2	1.045	0.942	0.205	0.024	1.125	0.803	0.772	0.095	0.008	0.564
Case 3	1.264	1.006	0.281	0.036	2.662	0.806	0.882	0.114	0.010	0.591
Case 4	1.065	1.235	0.211	0.049	0.712	0.914	0.911	0.118	0.013	0.596
Case 5	1.351	1.278	0.295	0.064	2.857	1.025	1.061	0.219	0.039	0.462
Case 6	0.916	0.871	0.131	0.078	1.131	0.795	0.698	0.098	0.051	0.486
Case 7	1.105	0.908	0.204	0.082	1.221	0.863	0.884	0.123	0.068	0.531
Case 8	1.112	1.014	0.304	0.097	2.236	0.904	0.939	0.186	0.071	0.562
Case 9	1.224	1.235	0.208	0.167	1.016	0.831	1.021	0.152	0.141	0.608
Case 10	1.338	1.263	0.315	0.182	2.253	1.002	1.085	0.245	0.153	0.628

Table 4(b): Feasible Assessment Indices (FAI) without and with HES unit (utilization factor K=0.75) for TATRIPS using PI^+ controller

Tatrips	Feasible Assessment Indices (FAI) based on control input deviations (ΔP_c) without HES unit (utilization factor K=0)					Feasible Assessment Indices (FAI) based on control input deviations (Δp_c) with HES unit (utilization factor K=0.75)				
	ε_1	ε_2	ε_3	ε_4	$\int P_{C1}$	ε_1	ε_2	ε_3	ε_4	$\int P_{HES}$
Case 1	0.912	0.856	0.123	0.014	1.011	0.861	0.796	0.078	0.010	0.468
Case 2	1.045	0.942	0.205	0.024	1.125	0.875	0.801	0.112	0.011	0.469
Case 3	1.264	1.006	0.281	0.036	2.662	0.877	0.913	0.123	0.014	0.525
Case 4	1.065	1.235	0.211	0.049	0.712	0.959	0.974	0.135	0.018	0.558
Case 5	1.351	1.278	0.295	0.064	2.857	1.201	1.105	0.248	0.044	0.451
Case 6	0.916	0.871	0.131	0.078	1.131	0.802	0.775	0.119	0.053	0.468
Case 7	1.105	0.908	0.204	0.082	1.221	0.928	0.886	0.136	0.073	0.528
Case 8	1.112	1.014	0.304	0.097	2.236	0.936	0.941	0.206	0.081	0.517
Case 9	1.224	1.235	0.208	0.167	1.016	0.938	1.049	0.178	0.149	0.545
Case 10	1.338	1.263	0.315	0.182	2.253	1.100	1.121	0.275	0.156	0.583

Table 4(c): Feasible Assessment Indices (FAI) without and with HES unit (utilization factor K=0.5) for TATRIPS using PI+ controller

	Feasible Assessment Indices (FAI) based on control input deviations (ΔP_c) without HES unit (utilization factor K=0)					Feasible Assessment Indices (FAI) based on control input deviations (ΔP_c) with HES unit (utilization factor K=0.5)				
Tatrips	ε_1	ε_2	ε_3	ε_4	$\int P_{C1}$	ε_1	ε_2	ε_3	ε_4	$\int P_{HES}$
Case 1	0.912	0.856	0.123	0.014	1.011	0.855	0.781	0.100	0.010	0.425
Case 2	1.045	0.942	0.205	0.024	1.125	0.871	0.808	0.128	0.018	0.448
Case 3	1.264	1.006	0.281	0.036	2.662	0.900	0.916	0.139	0.020	0.521
Case 4	1.065	1.235	0.211	0.049	0.712	0.945	0.945	0.148	0.021	0.538
Case 5	1.351	1.278	0.295	0.064	2.857	1.179	1.101	0.261	0.052	0.439
Case 6	0.916	0.871	0.131	0.078	1.131	0.798	0.771	0.122	0.062	0.461
Case 7	1.105	0.908	0.204	0.082	1.221	0.928	0.878	0.165	0.071	0.486
Case 8	1.112	1.014	0.304	0.097	2.236	0.935	0.954	0.231	0.078	0.489
Case 9	1.224	1.235	0.208	0.167	1.016	0.923	1.109	0.179	0.158	0.534
Case 10	1.338	1.263	0.315	0.182	2.253	1.100	1.127	0.289	0.162	0.542

Table 4(d): Feasible Assessment Indices (FAI) without and with HES unit (utilization factor K=0.25) for TATRIPS using PI+ controller

	Feasible Assessment Indices (FAI) based on control input deviations (ΔP_c) without HES unit (utilization factor K=0)					Feasible Assessment Indices (FAI) based on control input deviations (ΔP_c) with HES unit (utilization factor K=0.25)				
Tatrips	ε_1	ε_2	ε_3	ε_4	$\int P_{C1}$	ε_1	ε_2	ε_3	ε_4	$\int P_{HES}$
Case 1	0.912	0.856	0.123	0.014	1.011	0.858	0.783	0.110	0.014	0.397
Case 2	1.045	0.942	0.205	0.024	1.125	0.901	0.821	0.146	0.016	0.414
Case 3	1.264	1.006	0.281	0.036	2.662	0.951	0.912	0.187	0.024	0.425
Case 4	1.065	1.235	0.211	0.049	0.712	0.961	0.951	0.150	0.040	0.521
Case 5	1.351	1.278	0.295	0.064	2.857	1.293	1.136	0.262	0.061	0.396
Case 6	0.916	0.871	0.131	0.078	1.131	0.810	0.800	0.131	0.067	0.441
Case 7	1.105	0.908	0.204	0.082	1.221	0.943	0.879	0.172	0.082	0.459
Case 8	1.112	1.014	0.304	0.097	2.236	0.956	0.961	0.253	0.086	0.444
Case 9	1.224	1.235	0.208	0.167	1.016	0.936	1.109	0.185	0.171	0.493
Case 10	1.338	1.263	0.315	0.182	2.253	1.200	1.156	0.291	0.180	0.497

Table 5(a): Comprehensive Assessment Indices (CAI) without and with HES unit (utilization factor K=1) for TATRIPS using PI+ controller

	Comprehensive Assessment Indices (CAI) based on control input deviations (ΔP_c) without HES unit (utilization factor K=0)					Comprehensive Assessment Indices (CAI) based on control input deviations (ΔP_c) with HES unit (utilization factor K=1)				
Tatrips	ε_5	ε_6	ε_7	ε_8	$\int P_{C1}$	ε_5	ε_6	ε_7	ε_8	$\int P_{HES}$
Case 11	1.125	1.423	0.341	0.286	1.098	1.001	1.237	0.301	0.235	0.498
Case 12	1.511	1.411	0.378	0.335	3.188	1.081	1.343	0.310	0.301	0.594
Case 13	1.323	1.526	0.425	0.486	1.785	1.001	1.418	0.371	0.417	0.571
Case 14	1.536	1.635	0.451	0.508	3.172	1.427	1.551	0.382	0.474	0.588

Table 5(b): Comprehensive Assessment Indices (CAI) without and with HES unit (utilization factor =0.75) for TATRIPS using PI+ controller

	Comprehensive Assessment Indices (CAI) based on control input deviations (ΔP_c) without HES unit (utilization factor K=0)					Comprehensive Assessment Indices (CAI) based on control input deviations (ΔP_c) with HES unit (utilization factor K=0.75)				
Tatrips	ε_5	ε_6	ε_7	ε_8	$\int P_{C1}$	ε_5	ε_6	ε_7	ε_8	$\int P_{HES}$
Case 11	1.125	1.423	0.341	0.286	1.098	1.021	1.331	0.302	0.242	0.447
Case 12	1.511	1.411	0.378	0.335	3.188	1.101	1.410	0.319	0.305	0.528
Case 13	1.323	1.526	0.425	0.486	1.785	1.011	1.498	0.378	0.411	0.541
Case 14	1.536	1.635	0.451	0.508	3.172	1.436	1.598	0.400	0.481	0.547

Table 5(c): Comprehensive Assessment Indices (CAI) without and with HES unit (utilization factor K=0.5) for TATRIPS using PI$^+$ controller

Tatrips	Comprehensive Assessment Indices (CAI) based on control input deviations (ΔP_c) without HES unit (utilization factor K=0)					Comprehensive Assessment Indices (CAI) based on control input deviations (ΔP_c) with HES unit (utilization factor K=0.5)				
	ε_5	ε_6	ε_7	ε_8	$\int P_{C1}$	ε_5	ε_6	ε_7	ε_8	$\int P_{HES}$
Case 11	1.125	1.423	0.341	0.286	1.098	1.048	1.312	0.313	0.251	0.385
Case 12	1.511	1.411	0.378	0.335	3.188	1.189	1.421	0.321	0.310	0.448
Case 13	1.323	1.526	0.425	0.486	1.785	1.081	1.540	0.400	0.421	0.328
Case 14	1.536	1.635	0.451	0.508	3.172	1.478	1.611	0.404	0.492	0.467

Table 5(d): Comprehensive Assessment Indices (CAI) without and with HES unit (utilization factor K=0.25) for TATRIPS using PI$^+$ controller

Tatrips	Comprehensive Assessment Indices (CAI) based on control input deviations (ΔP_c) without HES unit (utilization factor K=0)					Comprehensive Assessment Indices (CAI) based on control input deviations (ΔP_c) with HES unit (utilization factor K=0.25)				
	ε_5	ε_6	ε_7	ε_8	$\int P_{C1}$	ε_5	ε_6	ε_7	ε_8	$\int P_{HES}$
Case 11	1.125	1.423	0.341	0.286	1.098	1.065	1.206	0.321	0.261	0.346
Case 12	1.511	1.411	0.378	0.335	3.188	1.140	1.284	0.328	0.305	0.420
Case 13	1.323	1.526	0.425	0.486	1.785	1.148	1.451	0.401	0.431	0.438
Case 14	1.536	1.635	0.451	0.508	3.172	1.341	1.529	0.414	0.497	0.445

inputs for the various case studies as shown in Table 1 and 2. The results are obtained by MATLAB 7.01 software and 100 iterations are chosen for the convergence of the solution using BFO algorithm. These PI$^+$ controllers are implemented in a Two-Area Thermal Reheat Interconnected Restructured Power System considering HES with Fuel Cell unit considering different utilization of capacity (K= 0, 0.25, 0.5, 0.75, 1.0) and for different type of transactions. The corresponding frequency deviations (Δf), tie- line power deviation (ΔP_{tie}) and control input deviations (ΔP_c) are obtained with respect to time as shown in Fig. 9-10. Simulation results reveal that the proposed PI$^+$ controller for the restructured power system coordinated with HES and fuel cell units greatly reduces the peak over shoot / under shoot of the frequency deviations and tie- line power flow deviation. And also it reduces the control input requirements and the settling time of the output responses are also reduced considerably is shown in Table 3.

Power System Ancillary Service Requirement Assessment Indices (PSASRAI)

Based on Settling Time:

- If ε_1, ε_2, ε_5, $\varepsilon_6 \geq 1$ then the integral controller gain of each control area has to be increased causing the speed changer valve to open up widely. Thus the speed- changer position attains a constant value only when the frequency error is reduced to zero.
- If $1.0 < \varepsilon_1$, ε_2, ε_5, $\varepsilon_6 \leq 1.5$ then more amount of distributed generation requirement is needed. Energy storage is an attractive option to augment demand side management implementation by ensuring the Ancillary Services to the power system.
- If ε_1, ε_2, ε_5, $\varepsilon_6 \geq 1.5$ then the system is vulnerable and the system becomes unstable and may even result to blackouts.

Based on Peak Undershoot:

- If $0.15 \leq \varepsilon_3$, ε_4, ε_7, $\varepsilon_8 < 0.2$ then Energy Storage Systems (ESS) for LFC is required as the conventional load-frequency controller may no longer be able to attenuate the large frequency oscillation due to the slow response of the governor for unpredictable load variations. A fast-acting energy storage system in addition to the kinetic energy of the generator rotors is advisable to damp out the frequency oscillations.
- If $0.2 \leq \varepsilon_3$, ε_4, ε_7, $\varepsilon_8 < 0.3$ then more amount of distribution generation requirement is required or Energy Storage Systems (ESS) coordinated control with the FACTS devices are required for the improvement relatively stability of the power system in the LFC application and the load shedding is also preferable
- If ε_3, ε_4, ε_7, $\varepsilon_8 > 0.3$ then the system is vulnerable and the system becomes unstable and may result to blackout.

CONCLUSIONS

This paper proposes the design of various Power System Ancillary Service Requirement Assessment Indices (PSASRAI) which highlights the necessary requirements that can be adopted in minimizing the frequency deviations, tie-line power deviation in a two-area Thermal reheat interconnected restructured power system in a faster manner to ensure the reliable operation of the power system. The PI^+ controllers are designed using BFO algorithm and implemented in a TATRIPS without and with HES unit. As the PI^+ control uses a low-pass filter on the command signal to remove overshoot. In this way, the integral gain can be raised to higher values for the load frequency applications. It has been proved that the PI^+ controller as it uses the command filter, attenuates the peaking caused by PI controller gains. BFO Algorithm was employed to achieve the optimal parameters of gain values of the various combined control strategies as BFO algorithm is easy to implement without additional computational complexity, with quite promising results and ability to jump out the local optima. Moreover, Power flow control by HES unit is also found to be efficient and effective for improving the dynamic performance of load frequency control of the interconnected power system than that of the system without HES unit. From the simulated results it is observed that the restoration indices calculated for the TATRIPS with HES unit indicates that more sophisticated control for a better restoration of the power system output responses and to ensure improved Power System Ancillary Service Requirement Assessment Indices (PSASRAI) in order to provide good margin of stability than that of the TATRIPS without HES unit. Moreover from the results it is evident that proper selection of the utilization factor of HES units in the TATRIPS the ancillary service requirement ($\int P$) can be optimistically be utilized.

ACKNOWLEDGEMENT

The authors wish to thank the authorities of Annamalai University, Annamalainagar, Tamilnadu, India for the facilities provided to prepare this paper.

REFERENCES

1. Omveer Singh, Prabhakar Tiwari, Ibraheem and Arunesh Kr. Singh, 2013. A Survey of Recent Automatic Generation Control Strategies in Power Systems. Int. J. Emer. Trends Electr. Electro. ISSN: 2320-9569, 7(2): 1-14.
2. Anupama, Dubey and Pallavi Bondriya, 2016. Literature Survey on Load-Frequency Controller. International Research Journal of Engineering and Technology (IRJET), 3(5): 1604-1611.
3. Kumar, P., S.A. Kazmi and N. Yasmeen, 2010. Comparative study of automatic generation control in traditional and deregulated power environment. World J. Model. Simu., 6(3): 189-7.
4. Shashi Kant Pandey, Soumya R. Mohanty and N. Kishor, 2013. A literature survey on load–frequency control for conventional and distribution generation power systems. Renew. Sust. Energy Rev., 25: 318-4.
5. Mukta, Balwinder Singh Surjan, 2013. Load Frequency Control of Interconnected Power System in Deregulated Environment: A Literature Review. Int. J. Eng. Adv. Tech. ISSN: 2249-8958, 2(3): 435-1.
6. Elyas Rakhshani and Javad Sadesh, 2010. Practical view points on load frequency control problem in a deregulated power system. Energy Convers. Manage., 51(5): 1148 -6.
7. Sivachandran, P., D. Lakshmi and R. Amalrajan, 2016. A Study on Load Frequency Control.Middle-East Journal of Scientific Research, 24(3): 740-9.
8. Bhatt, P., R. Roy and S.P. Ghoshal, 2010. Optimized multi area AGC simulation in restructured power systems. Electr. Power Energy Syst., 32: 311-22.
9. Chidambaram, I.A. and B. Paramasivam, 2013. Optimized Load- Frequency Simulation in Restructured Power System with Redox Flow Batteries and Interline Power Flow Controller. Electr Power Energy Syst., 50: 9-24.
10. Sterpu, S., Y. Besanger and N. Hadjsaid, 2005. Ancillary services performance control in deregulated power system. IEEE Power Eng. Soc., 3: 3048-4.
11. Rahi, J.O.P., Harish Kumar Thakur, Abhash Kumar Singh and Shashi Kant Gupta, 2013. Ancillary Services in Restructured Environment of Power System. Int. J. Innov. Tech. Res., ISSN: 2320-5547, 1(3): 218-5.
12. Dimitris Ipsakis, Spyros Voutetakis, Panos Seferlisa, Fotis Stergiopoulos and Costas Elmasides, 2009. Power management strategies for a stand-alone power system using renewable energy sources and hydrogen storage. Int. J. Hydrogen Energy, 34: 7081-95.
13. Ke´louwani, S., K. Agbossou and R. Chahine, 2005. Model for energy conversion in renewable energy system with hydrogen storage. J. Power Sources, 140: 392-9.

14. Robin Parker, William L, Clapper Jr. Hydrogen - based utility energy storage system. Proceedings of the 2001 DOE Hydrogen Program Review NREL/CP-570-30535.
15. Passino, K.M., 2002. Biomimicry of bacterial foraging for distributed optimization and control. IEEE Control Sys. Magazine, 22(3): 52-67.
16. Janardan Nanda, S. Mishra and Lalit Chandra Saikia, 2009. Maiden Application of Bacterial Foraging-Based optimization technique in multi-area Automatic Generation Control. IEEE Trans. Power Syst., 24(2): 602-9.
17. Peer, Mohamed M., E.A. Mohamed Ali and I. Bala Kumar, 2012. BFOA Based Tuning of PID Controller for a Load-Frequency Control in Four Area Power System. Int. J Commun. Engg. ISSN: 0988-0382E 2012; 3(2): 56-4.
18. George Ellis, 2004. Control System Design Guide. 3rd Edition. California: Elsevier Academic Press.
19. Fatemeh Daneshfar, 2013. Load-Frequency Control in a Deregulated Environment Based on Reinforcement Learning. Journal of Control and Systems Engineering, 1(1): 9-6.

Appendix A:

A1 Data for Thermal Reheat Power System [9]
Rating of each area = 2000 MW, Base power = 2000 MVA, f^o = 60 Hz, $R_1 = R_2 = R_3 = R_4$ = 2.4 Hz / p.u.MW, $T_{g1} = T_{g2} = T_{g3} = T_{g4}$ = 0.08 s, $T_{r1} = T_{r2} = T_{r1} = T_{r2}$ = 10 s, $T_{t1} = T_{t2} = T_{t3} = T_{t4}$ = 0.3 s, $K_{p1} = K_{p2}$ = 120Hz/p.u.MW, $T_{p1} = T_{p2}$ = 20 s, $\beta_1 = \beta_2$ = 0.425 p.u.MW / Hz, $K_{r1} = K_{r2} = K_{r3} = K_{r4}$ = 0.5, $2\pi T_{12}$ = 0.545 p.u.MW / Hz, a_{12} = -1.
A.2 Data for the HES unit [13]
K_{AE} = 0.002, T_{AE} = 0.5, K_{FC} = 0.01, T_{FC} = 4